scientific reports

Check for updates

OPEN

Model based ranking of the influence of geometry and materials on the dynamical behavior of the violin highlights predominance of geometrical choices

Romain Viala[1,2]✉, Vincent Placet[3], Emmanuel Foltête[4] & Scott Cogan[3]

When considering the vibroacoustical behavior of the family of violin instruments, especially related to their construction, numerous beliefs and theories coexist that are not necessarily compatibles between each other. More specifically, the resulting sound or dynamics of the instrument are associated to tonewood properties and geometry, but with ranking and weights that vary according to beliefs and testimony of makers. This study presents an approach to understanding the relative influence of both geometrical and material properties on the vibrational dynamics of the violin. By conducting a screening analysis, using finite element method based computations of a complete violin, we explore impact of maker's choices during the construction process. The results highlight that the dynamical behavior of the violin is mainly depending on geometrical choices, such as thickness of back and top plate or f-holes shapes, rather than the complete variability of properties of tonewoods. Therefore, the wood selection appears to be a second order effect compared to other luthier's choices, supporting a craftsmanship practice and can pave the way to the use of lower grade woods, which are more in adequacy with what the resource can offer. This work offers new insights that can assist violin makers in optimizing their design choices and adapting to sustainable material use without compromising subsequent behavior.

Keywords Musical acoustics, Virtual prototyping, Violin, Screening analysis, Tonewood

Almost forty years separate the "Acoustics of stringed instruments" article[1] and "The acoustics of the violin: a review"[2]. In this time interval, most of the elements proposed by the first reference have been rigorously studied, and more detailed models of, among others, bowed strings, violin acoustic radiation, and violin vibratory response have been developed. The development of physics-based numerical models of musical instruments has grown along with the computational capacities. However, methodological gaps remain for the study of the complex phenomena, such as the interactions between all the components of the violin.

From the operational point of view, the excitation is applied through a non-linear phenomenon of stick slip by the bow's hair on the string. The motion of the strings is coupled with the dynamic behavior of the bridge and the violin body which is made of numerous parts glued together as shown on Fig. 7. Among all the solids assembled together, many are carved or bent to complex shapes, that cannot all be studied by traditional analytical approaches or usual material characterization devices. Beyond the global shape of the violin, numerous inner elements and more specific designs have evolved through the centuries, such as the angle of its neck, the type of strings, and the bass bar shape.

[1]ITEMM-Institut Technologique Européen des Métiers de la musique, 71 avenue Olivier MESSIAEN, 72000 Le Mans, France. [2]Department of Applied Mechanics, Université de Franche-Comté, CNRS, institut FEMTO-ST, F-25000 Besançon, France, 25000 Besançon, France. [3]Department of Applied Mechanics, Université de Franche-Comté, CNRS, institut FEMTO-ST, F-25000 Besançon, France, Besançon 25000, France. [4]SUPMICROTECH, CNRS, institut FEMTO-ST, 25000 Besançon, France. ✉email: romain.viala@femto-st.fr

It is considered that the acoustic modes of the violin are particularly important on the projected sound below 1 kHz, and the violin behaves in this frequency range as a monopole[3]. But the overall response of the violin is not only linked to its acoustical modes, that are related to the acoustic behavior of its cavity[4,5], but also to the radiated sound of its structural components. The radiation of the instruments has been studied widely as reported in[6]. Almost fifty years ago, quantitative measurements have been performed on a violin, and the structural mode shapes at different frequencies have been described[7]. The experimental modal analysis, that has grown in popularity in the last decades, has therefore been widely applied to the violins. The laser speckle interferometry has been used for decades to observe the vibration modes of the components of the violin, especially its top and back shells[8] and the bodies[9]. Therefore, numerous experimental studies have identified vibroacoustic modes of the violin[5,10–14]. Finally, for more than 30 years, modal analysis has provided a nomenclature to different specific deformed shapes. These modes have been at the basis of the transfer of research results and had a favorable echo from the instrument makers, known as the plate-tuning method. A full detailed list of these modes and their indication for instrument making are given in[15–17] (Table 1 gives the nomenclature and brief description of modes) and studies propose correlations between the frequency of these signature modes and the sound and preference of violins[4,18]

Above and beyond the structural dynamics of the violin, numerous other features have been proposed, such as the sound radiation of the violin that has been proposed in[20], which defines the ratio between radiated sound field and the force applied on the bridge by the string, which is in the continuity of[21]. The frequency spectrum and directivity of the sound of the violin, which is a step beyond the acoustical and structural modes has also been studied[22]. In a more mixed analysis targeting a concrete application for violin makers, some parts of the response have been both experimentally and analytically linked to modifications of the violin components, such as the position of the soundpost, whose effect is given in[23], and simulated using a finite elements model of violin in[19]. This last study has also used the finite element models to determine the impact of the shape of the f-holes of the violin, which have been largely documented through centuries, with more and more advanced devices[24]. For higher frequency domains, the first studies focusing on the violin bridge vibrational properties have been performed several decades ago[9,25]. Thus, the bridge, by its own dynamics, filters the components of the motion of the string. Along with the different measures of the bridge admittance, this feature has been increasingly considered as a signature for violins, as the bridge admittance exhibits the dynamics of the bridge, but also of the soundboard it is attached to, i.e., the violin body. The study of violin bridge admittance[26] has shown a peak of response between 2000 and 3000 Hz. This feature has been called the "bridge hill" effect and is associated with motions of the violin bridge, especially in-plane bending, as shown in[27,28]. For assembled and finished instrument, violin varnishes influence the vibrational properties of of thin plates of wood, and their impact on dynamics has been studied this last decade, quantifying variations according to varnish type and wood preparation and grounding selected[29,30].

Even though all these methods may provide a complete characterization of the dynamical behavior of the instruments, they cannot be used directly to determine the impact of modifications of the geometrical and/or material properties that form the violin, due to strong aleatory uncertainties: the variability of the material[31] and surrounding conditions[32,33], and the properties of the glued interfaces that prevent consistent experimental studies with few samples, and the coarseness of analytical models. Moreover, experimental campaigns that study the impact of geometrical choices on finished instruments can be costly or particularly hard to achieve as the perceived sound can be attributed to many factors for which a geometrical or material choice is only a part[34,35]. In consequence, experimental and analytical studies have not yet consolidated knowledge about the link between specific maker choices and the resulting dynamical behavior of the instruments. Nevertheless, during the last decade, more and more studies have combined both experimental, analytical and numerical approaches to study musical instruments and to compare different shapes[36]. A study has used reverse engineering methods, experimental devices and numerical models of complete violin[37] to create a vibro-acoustic model of the violin the "Titian" made in 1715 by Antonio Stradivari. This approach combining geometry, material and sound in a detailed way is now in constant expansion. The finite element method has been used to calculate eigenmodes of a violin[38], modal frequencies on free violin plates after removal of wood on the bridge[39], and the influential material properties on violin plate frequencies[40] which was an important starting point to predict the impact of instrument maker crafting on the eigenfrequencies of the plates, as proposed in[41,42] using optimization methods.

Mode and usual frequency bandwidth	Description
TP (120–150 Hz)	Tailpiece frequency (vertical or twisting motion)
B-1 (145–190 Hz)	Body motion
A0 (260–290Hz)	"Coupled Helmholtz mode" or breathing acoustical mode
B0 (250–300 Hz)	Bending of neck
CBR (390–430 Hz)	Center bout rotation
B1- (or C2) (430–480 Hz)	Breathing of the body
A1 (430–490 Hz)	Internal cavity acoustical mode
B1+ (or C3) (510–580 Hz)	Bending of the body
W (450–550 Hz)	Main structure resonance when bowed
W' (225–275 Hz)	Subharmonic of W

Table 1. Nomenclature of the signature modes of the violin below 800 Hz, according to[17,19].

Using a finite element model, in free conditions, the link between structural eigenfrequencies and the material properties has been established in[43], which has also been studied for clamped conditions in[19] that studied the evolution of the mode shapes, from free to fixed conditions. Considering pragmatic expectations of violin makers, the impact of the f-hole shape has been investigated[44]. In[45,46], modeling and experimental approaches highlighted the impact of the shape of the f-hole on the acoustic radiation of the violin. Another perspective proposed early during the development of the finite element method was the capability of such methods to evaluate the material properties of the wooden parts used for violin making, in parallel with the modal analysis of these parts[47], which has been applied to tonewood (spruce quarters[48], and bear claw spruce[49]) or back and soundboard in[50,51] using both dynamical response and a finite element model.

Research aim

The aim of this study is to highlight which material or geometrical parameters impact the most the complex response of the violin, in the same way as proposed for guitar soundboards in[52]. To this end, a numerical model is developed for the study of the usual criteria used in the experimental and analytical characterization of the violins, namely the resonance mode shapes and frequencies, and the bridge admittance response amplitude (associated with the bridge hill effect). The complete numerical model proposed in this study aims at displaying full dynamical response of the violin up to 4000 Hz, even though the low frequency response will be emphasized with specific modes. This work is novel in its approach as it performs a systematic screening analysis that highlights the dominant influence of geometrical choices over material properties. This work also aims at offering practical results to violin makers, allowing them to prioritize steps during the crafting process and considering objectively materials without adversely affecting dynamical behavior.

Results

Computed vibrational modes and bridge admittance

The computed eigenmodes shapes and frequencies are displayed and the preliminary results are given. Figure 1 displays the deformed shapes of the violin body below 800 Hz (the chinrest and tailpiece of the violin are not displayed for better readability). The frequencies of the CBR (Center Bout Rotation, a torsion-like motion between the top and back plate with relatively low acoustic radiation[53]), B1−, B1+ (modes involving the in- and out-of-phase combinations of a bending and breathing mode[19]), and C4 modes are in accordance with the measured modes on real violins, given in Table 1 and that have been measured for decades in the acoustics of the violin domain[2,8,37,54]. The presented modes are considered in the screening analysis details and the most influential parameters on each mode separately are given. The maximum bridge admittance in the [1600 3000 Hz] frequency range is given in Fig. 2 and show that the mean bridge admittance maximum value is close to 0.022 mm/N, and its standard deviation is equal to 0.006 mm/N. The bridge admittance values vary by ±35% (± standard deviation σ), but can shift up to +250 % for several cases. Such particular configurations mostly involve the f-holes length and soundboard thickness, which are clues for the screening analysis of this features, and will be focused quantitatively below. The maximum value generally appears at 2400 ± 300 Hz. This frequency is coherent with the usual values of the center of the bridge hill[55–57] which supports these results.

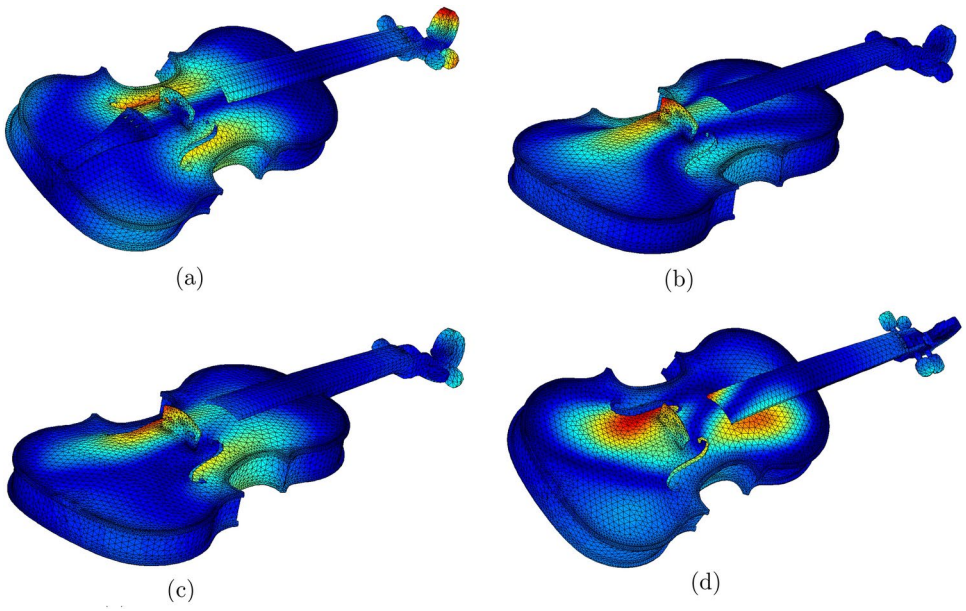

Fig. 1. Eigenmode shapes of the numerical modes of the violin body, no prestress included.

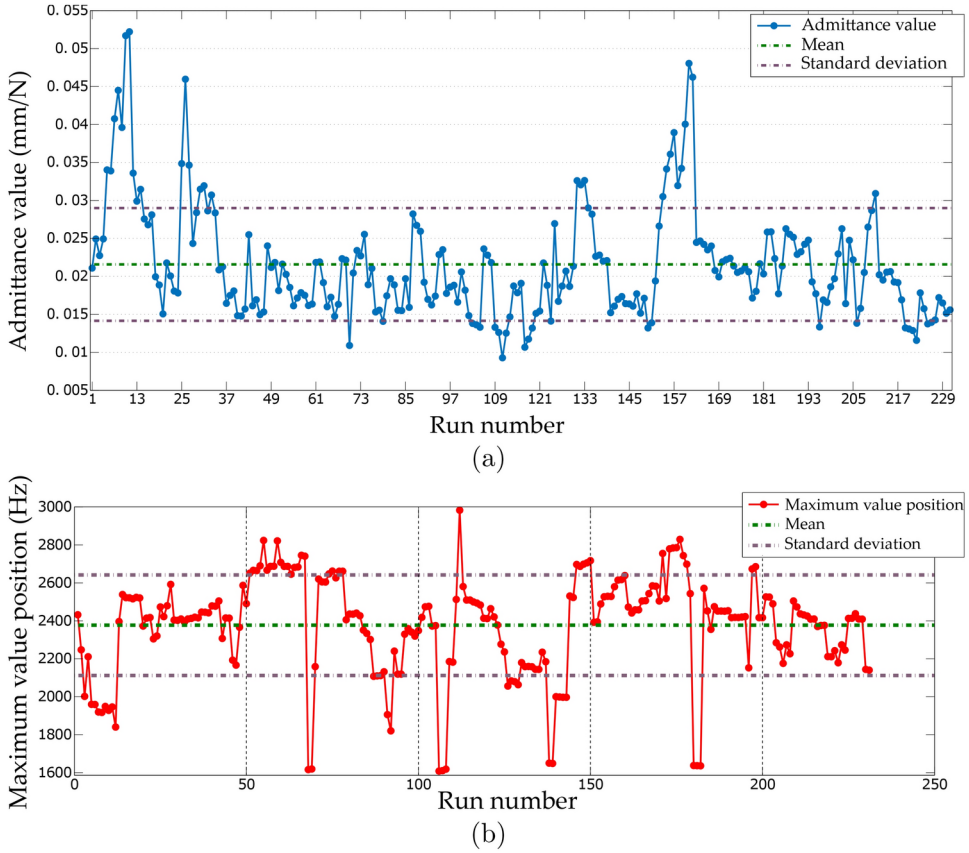

Fig. 2. Maximum frequency response function (FRF) amplitude (**a**) and frequency (**b**) in the [1600–3000 Hz] band.

Screening analysis results

The results of the screening analysis based on the 211 computations are presented in Figs. 3, 4, 5, 6. All the parameters are ranked according to their normalized elementary effects on the associated feature. The nomenclature is given in Table 6. It is shown that, according to the feature, the ranking of the parameters varies.

Global behavior

The maximum admittance per band is mainly sensitive to the soundboard (9.4 %) and back (12.5 %) thickness and associated densities, respectively 6.3 and 12.5 %. As these parts behave like vibrating plates, this result was expected, but a relative influence of each parameter is a new result. Moreover, this feature is also sensitive to the bridge cuts (6.3 %), which is coherent with the previous results and the f-holes length (13.5 %) which changes the global stiffness of the bridge/soundboard/f holes area. The remaining elastic parameters are weakly influential with respect to the thickness parameters especially, and in the same order of influence as density and small geometrical and presets changes. The global matched eigenfrequencies error (MEE) are mainly sensitive to the thickness (soundboard 24 %, back 14 %) and density (soundboard 8.3 %, back 12.5 %) of the plates, as expected, and the Young's modulus of the back in R direction (6.2 %), and the shear modulus of the soundboard (5.2 %). The maximum global admittance, which occurs near 400 Hz is sensitive to the position in the X direction and diameter of the soundpost (8.3 and 5.2 % respectively). Thus, the soundpost is a good way of tuning of the violin bridge admittance in this frequency domain, which is its usual but not necessarily explicated purpose. Thus, it seems that the position in the X direction of the soundpost is more important than the position in the Y direction on the dynamics of the violin. For better readability, the parameters are gathered into families and the results are given in Fig. 4. This Figure shows the higher impact of usual geometrical changes with respect to the material full variability for maximum admittances values in both [1600-3000] and [20-4000] Hz bands, and matched eigenfrequencies (46.3 to 56.8 % compared with 38.9 %). In addition, the movable presets also play a non-negligible role (5.3 to 14.7 %).

Signature modes

The parameters ranking for body, soundboard and back modes below 800 Hz are given in Fig. 5, and grouped in Fig. 6. It is shown that according to the considered modes, the parameter ranking differs. For the center bout rotation (CBR) mode, the density of the back is mainly significant (25 %), followed by the specific modulus in radial direction of the soundboard (18.7 %). The thickness of both back and soundboard are influential (11.5 % for each one). For the mode B1-, The thickness of the soundboard is mainly influential (33 %), followed by

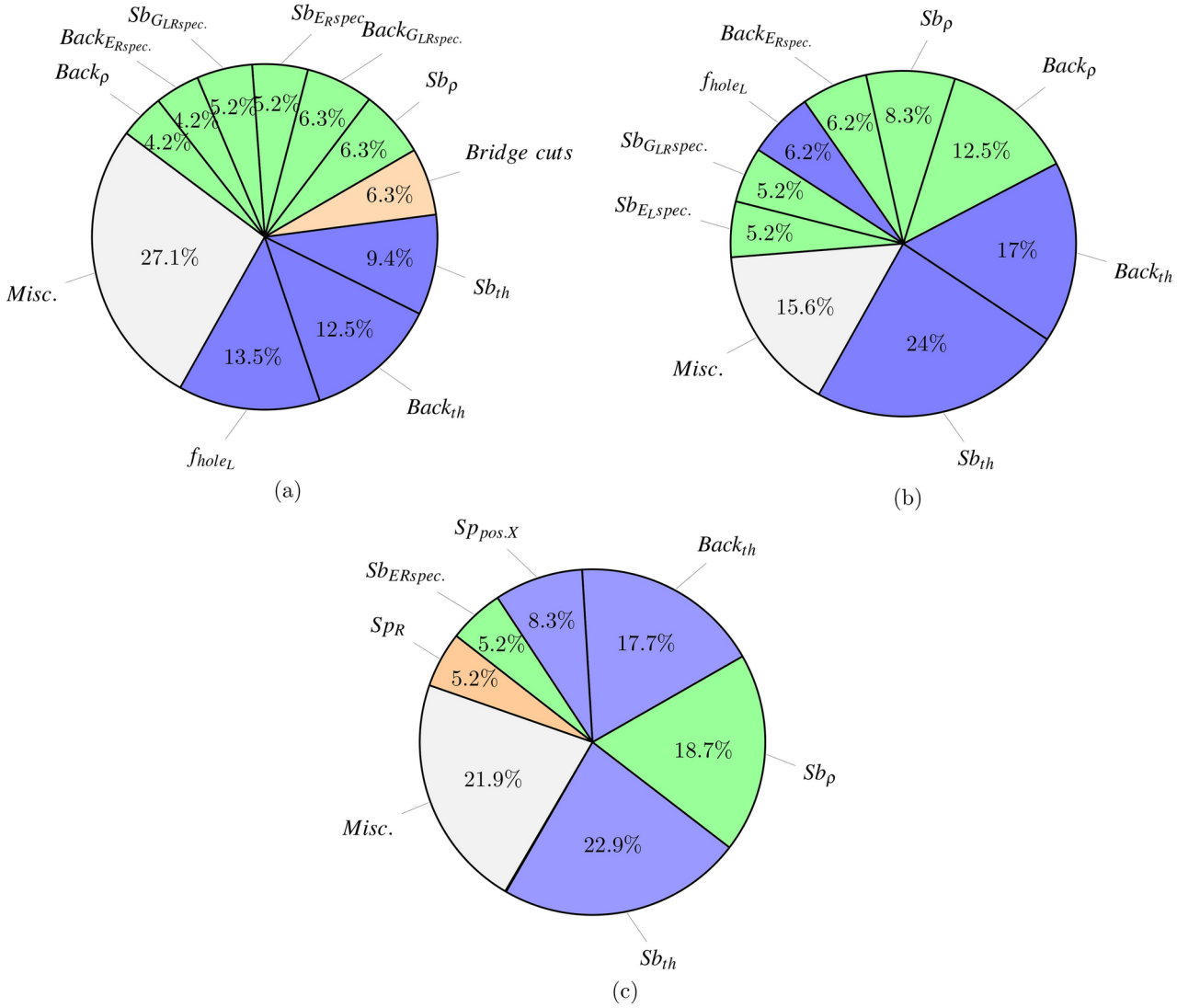

Fig. 3. Ranking of the parameters according to: (**a**) the maximum admittance in the bridge hill band [1600-3000 Hz] (**b**) all the matched eigenfrequencies (MEE) (**c**) overall maximum admittance [20–4000 Hz].

its density (15.5 %) and the soundpost position in X direction (7.2 %, across the width of the instrument). The back thickness and density are less influential (6.2 and 5.1 %). The longitudinal and radial specific moduli of soundboard are equally influential (5.1 %) . The B1+ (or C3) mode is influenced by soundboard and back thicknesses respectively (20.7 and 19.6 % respectively). Their densities are also influential (13 and 7.6 %). Finally, the radial specific modulus of the back (7.6 %) and longitudinal specific modulus of the soundboard (5.4 %) are also influential. The thickness of the back and soundboard are mostly influential on the eigenfrequencies of the presented modes. These results are in agreement with the propositions of Carleen Hutchins to tune the frequency of such modes[17] and thus can be a starting point for a more effective and focused plate tuning during the violin making, avoiding the uncertainty seen in the assembly process which was highlighted for a lute in[58]. The radial elastic modulus of the soundboard seems to have an impact on the frequency of the CBR mode, thus the utilization of bear claw spruce which exhibits a much higher stiffness in radial direction has been studied[49]. The eigenfrequencies are mainly sensitive to the thickness and density of the soundboard and the back, and the Young's modulus of the back in R direction and the LR shear modulus of the soundboard, and longitudinal rigidity of soundboard, which is consistent with the results of[59]. Finally, the length of the f-holes seems to be the most influential geometrical parameter (aside fromthe thicknesses) on the eigenfrequencies, as proposed in[46].

Discussion

Based on the proposed numerical model, the eigenfrequencies of a violin are mainly sensitive to the thickness and density of the plates, and the Young's modulus of the back in R direction and the shear modulus of the soundboard. In addition, the presets also play a significant role. The dominant influence of the geometry and preset choices of the instrument maker has thus been pointed out through this study. However, other factors, such as the arch height and shape, can also significantly influence the violin's dynamical behavior. These parameters

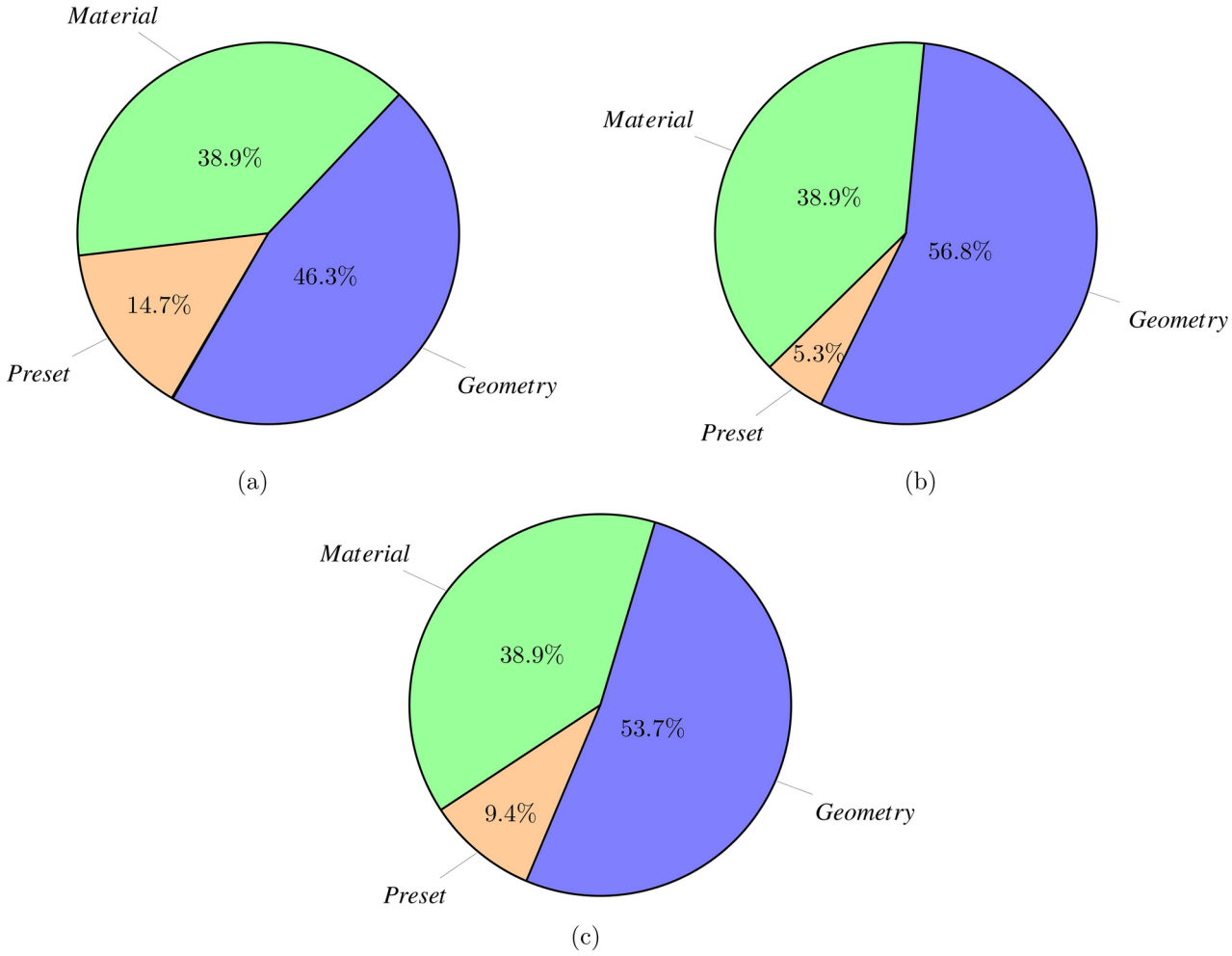

Fig. 4. Ranking of the grouped material, preset and geometrical parameters according to: (**a**) the maximum admittance in the band [1600-3000 Hz] (**b**) all the matched eigenfrequencies (MEE) (**c**) overall maximum admittance [20–4000 Hz].

were not included in the numerical model for two reasons. Primarily, the feasibility of changing arch shape in a parameterised model can lead to issues during the geometrical reconstruction. Secondly, the instrument maker generally uses templates to reach a desired arching shape and height. Therefore, for a given model, these parameters are less likely to change than those that have been studied here. However, the existing literature highlights that variations in arch height and shape do indeed affect the vibrational modes and sound projection of the instrument[60,61]. Future research should incorporate these factors to provide a more comprehensive understanding of the violin dynamics, whereas the focus of this study was to evaluate the instrument makers' choices. It has to be pointed out that including these parameters would increase the impact of geometry at the expense of material properties, supporting the importance of geometry rather than material. When considering separately the geometry, irreversible changes like thickness, and the presets, it is shown that presets also show an effect, which is a key to understanding impact of the instrument maker at different steps of construction process, especially the last one where tunable parts are added, as a mean to adapt the instrument. Finally, the violin in its final state is varnished and latter studies should also include the impact of varnish and wood preparation or grounding on the dynamics, increasing the variability of a violin body in its final step.

Application of findings to violin making

The findings have practical implications for violin craftsmanship. By demonstrating that geometrical parameters have a more significant impact on the violin's dynamical behavior than the variability of tonewood properties, luthiers can prioritize precise control over these dimensions during the construction process. This insight supports interest for alternative, more readily available, wood species or samples, without compromising the instruments acoustics, potentially reducing material costs and promoting sustainable practices in violin making. By understanding the influence of geometrical choices, material properties, and presets, luthiers can make more informed decisions about where to focus their craftsmanship efforts to achieve a desired dynamical behavior. Although plate tuning is common in violin making for plates in free boundary conditions, the proposed approach also helps to better anticipate and control clamped conditions. The significant impact of plate

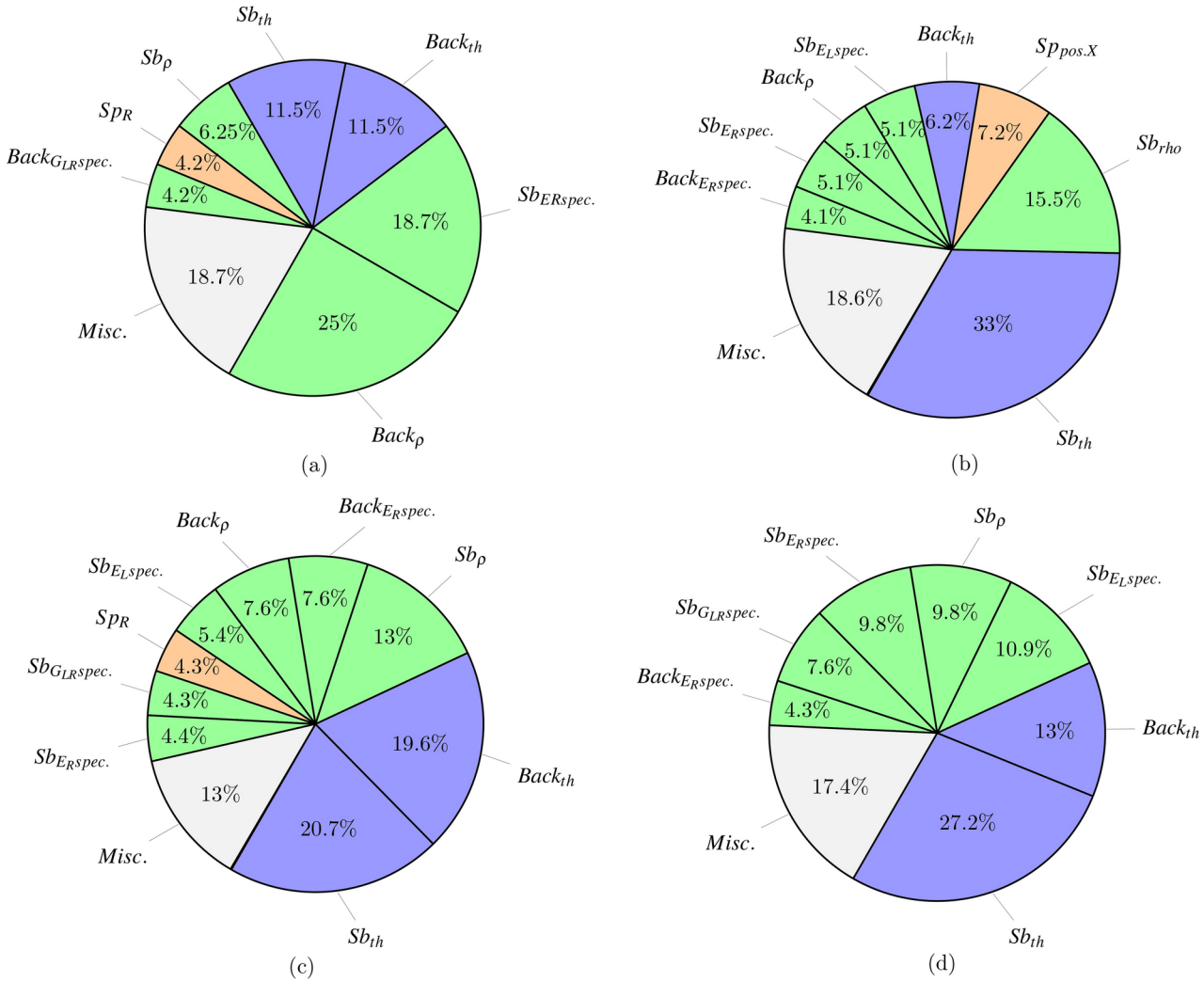

Fig. 5. Screening analysis of the parameters on the soundboard, back and body modes of the violin below 800 Hz. (**a**) CBR 390 Hz (**b**) B1- 432 Hz (**C**) B1+ 492 Hz (**d**) C4 top 680 Hz.

thickness reinforces the need for thickness calipers, arching templates, and gauges that luthiers have widely used. Additionaly, technologies such as 3D scanners, which are features present in smartphones with Light Detection And Ranging (LiDAR) or using photogrammetry, can be employed for fine geometry checks.

Regarding wood, affordable moisture meters can help assess wood moisture content, which is known to affect density and rigidity, and evaluate changes in these parameters in typical playing environments. Integrating knowledge of dynamical behavior can assist in measuring material properties based on longitudinal or flexural waves at the state of the wedge or samples, or even at the plate stage using the Finite Element Model Updating approach, which is already spreading in the violin-making community through online platforms with finite element computations. Variations in density or stiffness are common in instrument making, but as long as the geometric parameters are adapted, the overall impact will be less significant.

Elements such as the soundpost position, bridge shape, and other tunable parts also affect the behavior but are considered less influential than the primary geometric factors. However, these presets are crucial for final adjustments and fine-tuning after the main construction is complete. To influence the bridge hill effect and adjust the response of the violin in the [1600-3000 Hz] range, several parameters have been identified as particularly influential. Regular testing of the bridge's fitting and shape adjustments can be guided by the study's insights into bridge admittance. Moving the soundpost slightly adjusts the response of the instrument, and results show that the effect is more pronounced on B1- and B1+ modes, which can be controlled by makers.

Conclusion

The objective of this study was to highlight the usefulness of detailed physics-based models of musical instruments as a tool to test claims made by instrument makers or researchers. The dedicated model and associated computations showed that the geometrical choices of the maker represent dominant influence on the violin dynamics. The full variability of the material properties has a smaller impact on the dynamics than the several tenths of a millimeter changes that are dependent on the instrument maker choices, habits, experience

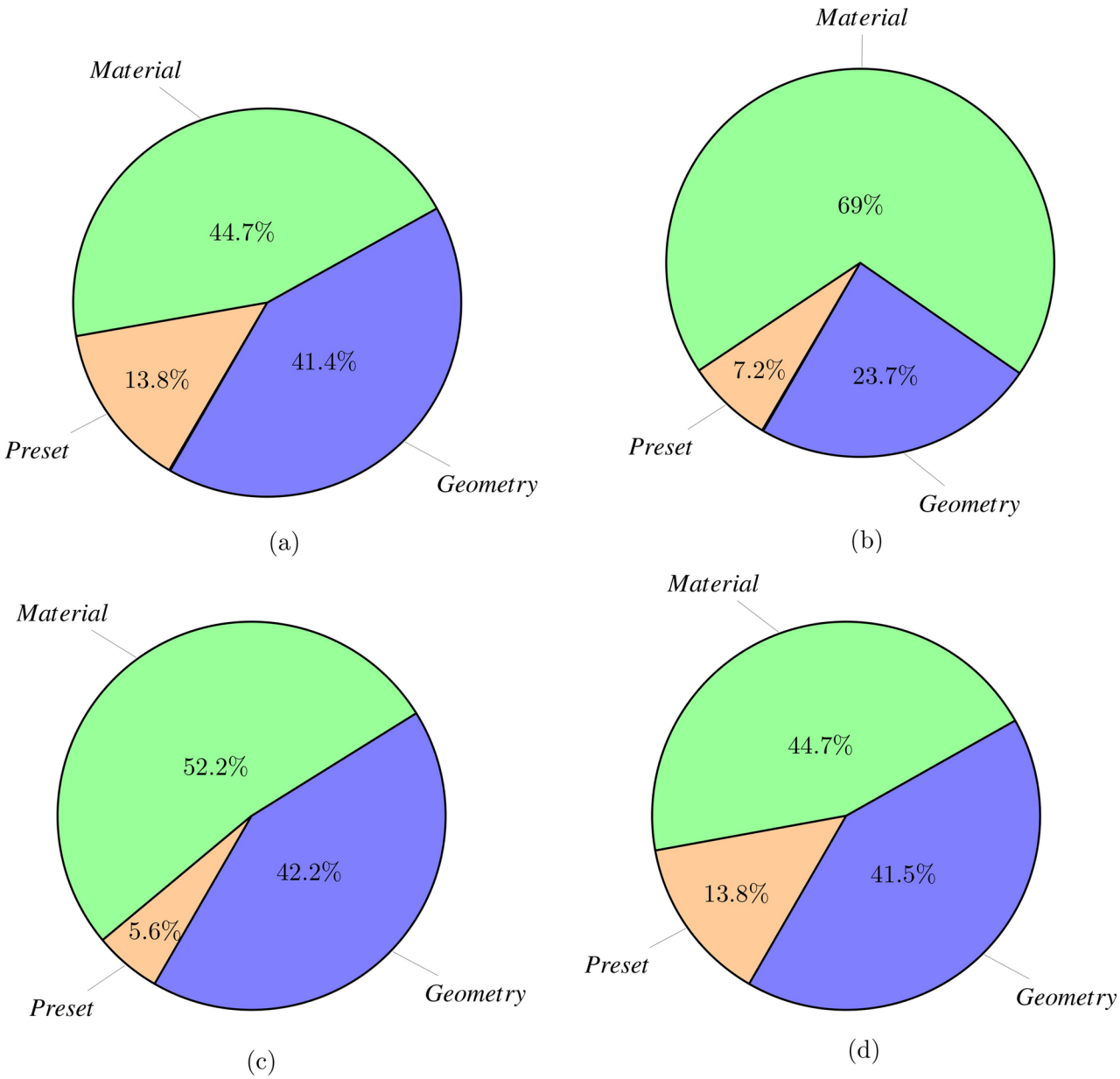

Fig. 6. Ranking of the grouped material, geometry and presets parameters according their influence on the back and body eigenfrequencies of the modes of the violin below 800 Hz. (**a**) CBR 390 Hz (**b**) B1- 432 Hz (**C**) B1+ 492 Hz (**d**) C4 top 680 Hz.

or crafting uncertainties. Nevertheless, the importance of these choices depends on the features considered. One of the main perspectives of such models, and considering the main influence of the thickness, is to optimize the thickness distribution of the parts to attain the desired acoustical properties, as proposed in[62] and applied in[41,42,63] for the optimization of free plates. In addition, it would also be possible to adapt the geometry in the case of wood modifications or substitution[64] or the proposal of new materials, thus requiring a geometry update. This study is pertinent in a dynamical domain allowing the clear identification of eigenmodes. At higher frequencies, the observation of single modes is complicated by the frequency and/or the damping coupling, which prevents the study of the violin behavior with modal analysis. Therefore, the study of bridge admittance in a broad frequency range would be more fruitful, as a broader indicator. In addition, descriptors used in the statistical energy analysis (SEA) method would also be useful when mixing both approaches. Finally, a main application of this approach would be the correlation with perception like in[34,65], and the use of sound synthesis based on these models to achieve a repeatability that can hardly be achieved with real instruments and players.

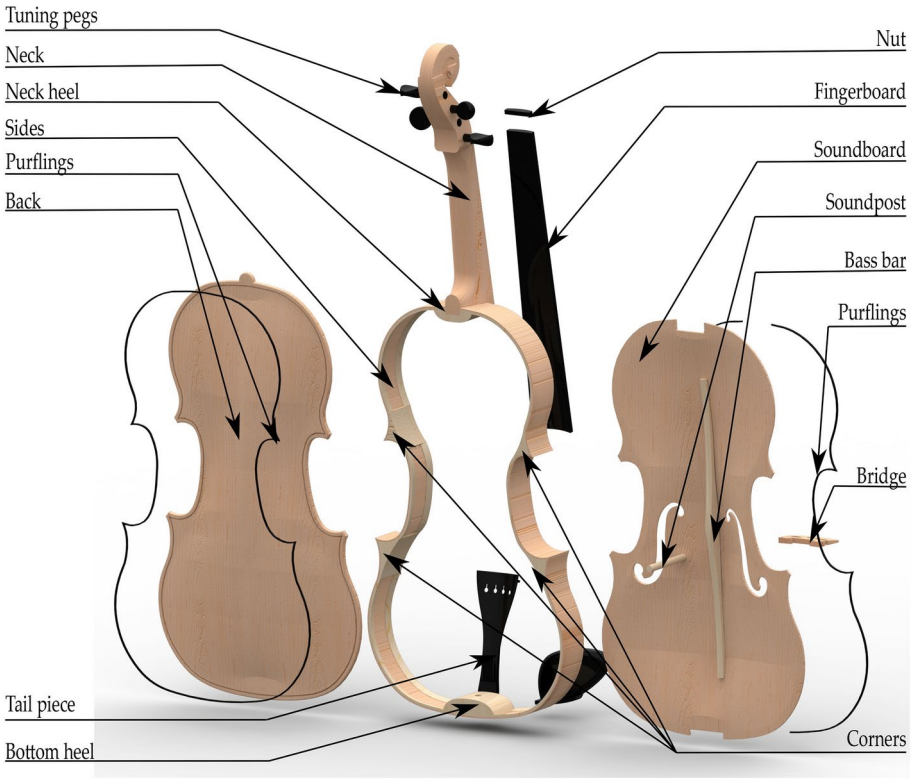

Fig. 7. Nomenclature of the violin.

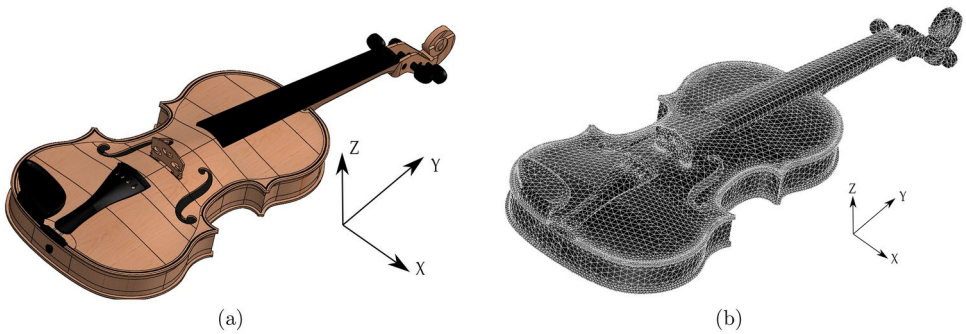

Fig. 8. (**a**) Computer aided designs of the violin as displayed in the CAD software ; (**b**) tetrahedral meshing of the violin and close up of the soundboard.

Material and methods

Computer aided design

The model developed corresponds to a fully mounted violin, and includes the tailpiece, bridge, chinrest and tuning pegs. The computer aided design (CAD) of the model is based on wooden molds and jigs of an instrument maker of the earliest twentieth century, Maurice Fauconnier. All the different solids used for the making of the violin are detailed in Fig. 7. Figure 8a displays the same model in a non-rendered view. The splines used for the making of the model are clearly visible on the soundboard and sides. Once the CAD of the violin has been made, different parts have been configured.

Configurable geometry

Two different kinds of tunable geometrical parameters are considered in this study. First, there are the parameters that cannot be easily changed once the violin is built (e.g., the thickness of the soundboard, the properties of the bass bar and the shape of the f-holes). Secondly, there are the parameters that are considered as presets and adjustable by the instrument maker, such as the position of the soundpost and the shape of the bridge. This set of geometrical modifications is not exhaustive but constitutes a starting point, as the effects of these parameters have long been a source of intrigue for instrument makers. Figure 10 (a) displays a cutaway view of

the violin in the XY plane. This Figure displays the different parameterized elements, such as the position of the soundpost in the X and Y direction and the length, width and position of the bass bar. The f-holes are displayed in Fig. 10(b). The width and length of the f-holes are also parameterized. The mean values of the parameters and their variation range are given in Table 2. The geometry is parameterized using a SOLIDWORKS feature called family tree. During the preparation of the CAD, some dimensions are selected to be dependent on the values gathered in an EXCEL sheet. The cells of this document are then modified during the study via MATLAB. After changes in the cells of the EXCEL table linked with SOLIDWORKS, the model is opened and reconstructed automatically, considering the modifications. A script, written in Python 2.7 is executed to send instructions to SOLIDWORKS. This method uses Pywin32 which is a Python extension for Windows application programming interface (API), that uses the component object model (COM) method. This step serves to export the updated model to a CAD format, parasolid (.x_t) that will be imported in the software MSC-PATRAN, the pre-processor used for the application of the finite element method.

Numerical model and mesh

Once the CAD model is prepared, configured and exported, a numerical model is automatically constructed using the finite elements method based on the commercially available software MSC-PATRAN. The mesh is created using quadratic tetrahedral elements of 5 mm as global edge length, whose dimensions are no more than a sixth of the wavelength for plate flexural waves at 4000 Hz and 3.5 mm thickness in longitudinal (E = 12 GPa) and radial (E = 1 GPa) directions, respectively 9 and 5 centimeters. Orthotropic material parameters are defined based on the results of[48,66,67]. Following the preprocessing of the model and the corresponding mesh, the number of elements is equal to 106000 which gives 300000 degrees of freedom. The mesh is created with a feature of MSC-PATRAN that creates elements with coincident faces for matched faces rather than adding contact parameters. The mesh refinement was performed automatically around the edges and near the purflings as represented in Fig. 8 (b). The modal basis is computed using the SOL103 solution in MSC-NASTRAN, which correspond to Normal Modes/Eigenvalue Analysis using the Lanczos Method[68] an iterative algorithm used for finding the eigenvalues and eigenvectors of large, sparse matrices The equation of motion for the violin structure undergoing free vibration is given by:

$$[M]\{\ddot{u}(t)\} + [K]\{u(t)\} = 0 \tag{1}$$

With $[M]$ and $[K]$ the mass and stiffness matrices respectively and $u(t)$ the displacement. Assuming a harmonic solution $\{u(t)\} = \{\phi\}e^{i\omega t}$, we get:

$$[M]\{-\omega^2\{\phi\}\} + [K]\{\phi\} = 0 \tag{2}$$

With ϕ the eigenvectors of the system and ω the pulsation. This leads to the eigenvalue problem that is solved:

$$([K] - \omega^2[M])\{\phi\} = 0 \tag{3}$$

Orthotropic material behavior laws and properties

All of the violin parts are assumed here to be made of wood, mainly spruce and maple for the body and the neck, and ebony for the fingerboard, chinrest, tailpiece and tuning pegs. The material parameters associated with the different parts of the violin are the Young moduli in i direction E_i, the shear moduli G_{ij} and the Poisson ratios ν_{ij}. A linear elastic orthotropic definition for each part of the violin is used, which gives 9 elastic parameters + density for each set of parts (the same material is considered for sides or ribs as if it was made from the same part of wood which is usually the case). The orthotropic consideration was the minimum that could be used to correctly consider the wood directions (L: longitudinal, R: radial and T: tangential). They are implemented in

Parameter	Nom. value (mm)	Min value (mm)	Max. value (mm)	Min. relative value (%)	Max relative value (%)
Length f-hole	73	69	77	- 5.5	+ 5.5
Width f-hole	42.5	40	45	- 6	+ 6
Width bar	6.1	5	6.5	- 0.22	+ 6.5
Position bass bar	9.5	8	11	- 16	+ 16
Length bass bar	270	290	250	- 7.4	+ 7.4
Height bass bar	11.1	9	16	- 23	+ 31
Radius soundpost	3	2.5	3.25	- 16	+ 8
Position X soundpost	15.6	14	18	- 10	+15
Position Y soundpost	8	5	11	- 37	+ 37
Thickness soundboard	2.8	2.4	3.2	- 14	+ 14
Thickness back	2.95	2.7	3.4	-8	+15
Profile bridge	10	7	11	-30	+10

Table 2. Mean and relative values of the configurable parameters, and relative variation in comparison with nominal (nom.) value.

the model and a previous screening analysis has been performed in an earlier study[59] to determine the most influential material parameters. Out of a total of more than 100 material parameters, a subset of 8 parameters has been retained for the sensitivity analysis (soundboard and back E_L, E_R, G_{LR} and their specific gravity). The remaining parameters displaying a relatively weak impact have been fixed and taken from[67]. The subset of influential parameters has been identified from 40 wood samples using a numerical-experimental inverse method[48]. Table 3 gives the initial material properties for all the elements of the violin in their respective local coordinate frame. These parameters are taken from[67] and the results of[48]. For tropical woods, those values are extrapolated from[67] and can be refined using the ones proposed in[69]. Numerous different orientations are implemented, and the violin is generally made of solids in five different orientations and three wood species. The orientation is considered, since the anisotropy ratio of the wood is high and can reach a value of 20 or more, for softwoods. The components are oriented in different ways, for both aesthetic, structural and workability considerations. The orientation and wood species of each solid are given in Table 4 and represented in Fig. 9. On usual violins, the parts are carved except for ribs and sides that are bent. The orientation of the material properties is defined through the local coordinate frames of the elements inside each solid and oriented to match the correct orientation in the global coordinate frame, and the cut of the grain is considered for carved parts. The sides and linings of a violin, represented in Fig. 7 are made of bent wood. The sides are made with maple and the linings with spruce. These wood parts are briefly immersed in water and bent using a hot iron at a temperature ranging between 200 and 250°C, depending on instrument maker habits and the wood properties. Thus, only

LRT Ebony	
Material parameter	**Value**
E_L (MPa)	17000
E_R (MPa)	1960
E_T (MPa)	1110
ν_{LR}	0.37
ν_{RT}	0.65
ν_{TL}	0.032
G_{LR} (MPa)	1370
G_{RT} (MPa)	360
G_{TL} (MPa)	950
ρ (g/cm3)	1
LRT spruce	
Material parameter	**Value**
E_L (MPa)	13350
E_R (MPa)	1080
E_T (MPa)	680
ν_{LR}	0.38
ν_{RT}	0.49
ν_{TL}	0.02
G_{LR} (MPa)	930
G_{RT} (MPa)	40
G_{TL} (MPa)	812
ρ (g/cm3)	0.44
LRT Maple	
Material parameter	**Value**
E_L(MPa)	14920
E_R (MPa)	1960
E_T (MPa)	1110
ν_{LR}	0.37
ν_{RT}	0.65
ν_{TL}	0.032
G_{LR} (MPa)	1370
G_{RT} (MPa)	360
G_{TL} (MPa)	950
ρ (g/cm3)	0.64

Table 3. Fixed material properties values for different wood species and orientations. The values for ebony are taken from[67] and the results for spruce and maple are taken form[48,66].

Solid	Material	Orientation (LRT)	Remark
Back	Maple	RLT	Often carved, factory instruments may be bent
Bass bar	Spruce	RLT	Carved and adjusted to soundboard
Bridge	Maple	LTR	Carved from a shaped part
Button	Ebony	RLT	Part provided by supplier
Chinrest	Ebony	LRT	Part provided by supplier
Corners	Spruce	TRL	Carved to fit with outer shape
Fingerboard	Ebony	RLT	Carved to create an ergonomic shape
Heels	Spruce	RTL	Carved to fit violin shape and neck heel
Linings	Spruce	LRT	Bent and glued on sides
Neck	Maple	TLR	Carved to create a scroll and ergonomic shape
Nut	Ebony	LRT	Carved to support strings
Pegs	Ebony	LRT	Part provided by supplier and adjusted
Purflings	Maple	LRT	Bent and glued in the soundboard and back
Saddle	Ebony	LRT	Carved to support tailgut
Sides	Spruce	LRT	Bent to fit outer shape
Soundboard	Spruce	RLT	Often carved, factory instruments may be bent
Soundpost	Spruce	TRL	Adjusted to fit between soundboard and back
Tailpiece	Ebony	RLT	Part provided by supplier
Tailgut (tailpiece string)	Nylon	Isotropic	Part provided by supplier

Table 4. Wood species and orientation of the components of the violin in the global coordinate frame XYZ. Longitudinal: L, Radial: R, Tangential: T.

Fig. 9. Scheme of the material orientation of the parts in the violin.

the sides and linings are the bent parts of the model. For 3D tetrahedral elements, the orientation of the material constituting the bent parts is a non-trivial step. The software MSC-PATRAN®contains an option labeled "align solid elements" that enables the orientation of the numerous solid elements of a piece according to the normal of a surface and the alignment with a curve.

Material variability implementation

The variations of the spruce and maple properties are taken from the results of[48], and ([67]). The elastic parameters, highlighted to be particularly influential on the vibratory behavior of the violin body in[59], are given as a function of the density for spruce wood (at 10 % MC) in the Eq. (4):

$$E_{L_{\rho_0}} = 13000 + 45000 \times (\rho_0 - 0.45); E_{R_{\rho_0}} = 1000 + 5500 \times (\rho_0 - 0.45); G_{LR_{\rho_0}} = 840 + 1320 \times (\rho_0 - 0.45) \quad (4)$$

In the case of the maple wood, the mechanical parameters are expressed as a function of the density by the Eq. 5 ([67]):

$$E_{L_{\rho_0}} = E_{L_0} \times (\frac{\rho_0}{0.64})^{1.30}; E_{R_{\rho_0}} = E_{R_0} \times (\frac{\rho_0}{0.64})^{1.03} \quad (5)$$

In practice, wood exhibits significant variability in mechanical properties, even for a given density, due to different characteristics, natural growth patterns, microstructural characteristics such as the orientation of microfibrils, subtle variations in grain structure or special patterns used in musical instrument making (like bear claws spruce, or bird's eye or flamed maple). This is particularly relevant when modeling tonewood, which is sensitive to these variations across longitudinal, and radial (or tangential) directions. It is a common fact that Longitudinal and (to a lower extent) radial elasticity moduli can be expressed as a function of density linearly. The variations in wood stiffness are indeed due to density at first order and microfibril angle (MFA) at second order but there remain variations that can still persist even for a given density and MFA. This study consists of a one at a time analysis to evaluate effects at first order. To avoid high density and very low E_L which would not be physical, the variations on $\frac{E_L}{\rho}$ are applied then ρ is set, either at its nominal value or changed according to the values sampled by the method. The variations of specific moduli, for a given density is therefore implemented to explore the full spectrum of possible mechanical responses that might arise from such variations.

To ensure coherence in the orthotropic elasticity matrix when varying the elastic moduli, the Poisson's ratios are adjusted in a manner that maintains the required physical relationships. In particular, the relationships between Poisson's ratios and Young's moduli in each direction are preserved to satisfy the symmetry conditions inherent in orthotropic materials, specifically with the following conditions:

$$\frac{\nu_{LR}}{E_L} = \frac{\nu_{RL}}{E_R}, \frac{\nu_{LT}}{E_L} = \frac{\nu_{TL}}{E_T}, \quad \frac{\nu_{RT}}{E_R} = \frac{\nu_{TR}}{E_T}$$

This ensures that when either E_L or E_R is modified, the Poisson's ratios ν_{LR} and ν_{RL} are adjusted accordingly. This proportional relationship between Poisson's ratios and elastic moduli ensures that the components of the elasticity tensor remain congruent and physically meaningful. Similar relationships are also maintained for the other directions.

Screening analysis

The model is used to perform a screening analysis of the different materials and geometrical parameters detailed above. The Morris method is used[70], and 12 geometrical parameters, 8 material parameters (the material properties of neck and fingerboard are not considered) are studied. The bounds of the parameters are given in Table 5. The geometrical entities that are considered are given in Table 6 and their correspondence with the violin geometry schematized in 10.

In total, 20 parameters are activated. The number of runs is equal to : $((20 + 1) * N_t) + 1$, with N_t the number of trajectories. In this study, ten trajectories and six levels are considered, which lead to a total of 211 runs. The number of levels defines the discretization of the input space and impacts the resolution of the elementary effects for each parameter. As the number of levels is a balance between computational efficiency and sensitivity resolution, 6 levels are commonly used in the Morris method when the primary goal is to identify influential factors as this study aims at providing results at first order rather than conduct a full factorial analysis. Highlighting more subtle results would require more sophisticated approaches, as an example to highlight coupling effects, in this case combining Morris with sequential sampling strategy[71] would be more adapted and enable to search for finer effects for some sets of parameters that change drastically the behavior.

Dynamical features

A linear modal analysis labeled as *sol103* in the software is performed. The duration of a run is generally equal to 1 hour, on a core i3 with 8 GB RAM. For the post-processing of the model and application of Morris sensitivity analysis method, features and metrics are required, which are more detailed below.

Bridge admittance

The admittance of the bridge consists in the ratio between the output displacement on a point resulting from an input force as a function of the frequency. It is a frequency response function (FRF) based on the displacement. The FRF that is synthesized is based on the modal basis, and the modal superposition method is used which

Parameter	Mean	Relative min.	Relative max.	Actual min.	Actual max.
	[MPa]	[%]	[%]	[MPa]	[MPa]
Maple					
$\frac{E_L}{\rho}(MPa)$	23282	-20	+20	18643	27980
$\frac{E_R}{\rho}(MPa)$	3062	-28	+30	2205	3981
$\frac{G_{LR}}{\rho}(MPa)$	2148	-23	+30	1655	2792
Density	0.64	-20	+12	0.512	0.717
Spruce					
$\frac{E_L}{\rho}(MPa)$	12790	-30	+22	20350	35463
$\frac{E_R}{\rho}(MPa)$	980	-34	+65	1470	3675
$\frac{G_{LR}}{\rho}(MPa)$	820	-33	+32	1248	2459
$\rho(g.cm^{-3})$	0.44	-11	+15	0.39	0.504

Table 5. Variability of the materials implemented for Morris screening analysis, with actual, min and max values, based on[67] (maple) and[48,66] for spruce.

Label	Description	Remarks
Sb_{th}	Soundboard thickness	Adjusted by violin maker generally before assembly
$Back_{th}$	Back thickness	Adjusted by violin maker generally before assembly
f_{hole_L}	f-holes length	Adjusted before assembly
f_{hole_W}	f-holes width	Adjusted before assembly
Bar_{pos}	Position of the bass bar	Glued after carving the soundboard
Bar_h	Height of the bass bar	Adjusted on the soundboard
Bar_W	Width of the bass bar	Adjusted before assembly
Bar_L	Length of the bass bar	Adjusted before assembly
Bridge cut	Opening on each side of the arm	Cut by the luthier during fitting
$Sp_{pos.}X$	Soundpost position in X direction	Adjusted with a soundpost setter
$Sp_{pos.}Y$	Soundpost position in Y direction	Adjusted with a soundpost setter
$Sp_{diam}Y$	Soundpost diameter	Diameter selected before fitting
$Sb_{E_L spec}$	Specific rigidity of top in L direction	Wood selection
$Sb_{E_R spec}$	Specific rigidity of top in R direction	Wood selection
$Sb_{G_{LR} spec.}$	Specific rigidity of top in GLR plane	Wood selection
Sb_ρ	Density of soundboard	Wood selection
$Back_{E_L spec.}$	Specific rigidity of back in L direction	Wood selection
$Back_{E_R spec.}$	Specific rigidity of back in R direction	Wood selection
$Back_{G_{LR} spec.}$	Specific rigidity of back in GLR plane	Wood selection
$Back_\rho$	Density of back	Wood selection
Misc.	Miscellaneous	All weakly influential parameters gathered

Table 6. Nomenclature of the parameters used for the screening analysis results display.

involves summing the contributions of individual vibration modes, each represented by its corresponding eigenfrequency and mode shape. The equation governing the FRF is given by:

$$FRF(\omega) = \sum_{n=1}^{N} \frac{\phi_n \phi_n^T}{\omega_n^2 - \omega^2 + 2i\zeta_n \omega_n \omega}$$

where ϕ_n is the mode shape (eigenvector) of the n-th mode, ω_n is the natural frequency of the n-th mode, ζ_n is the damping ratio for the n-th mode, and ω is the excitation frequency. The modal damping that has been used is based on the modal damping evaluated with the data of real violins by means of laser 3D vibrometry[66], whose average value is $\zeta_n = 0.9\%$. Once the modal basis of the full mounted violin is computed, the screening analysis

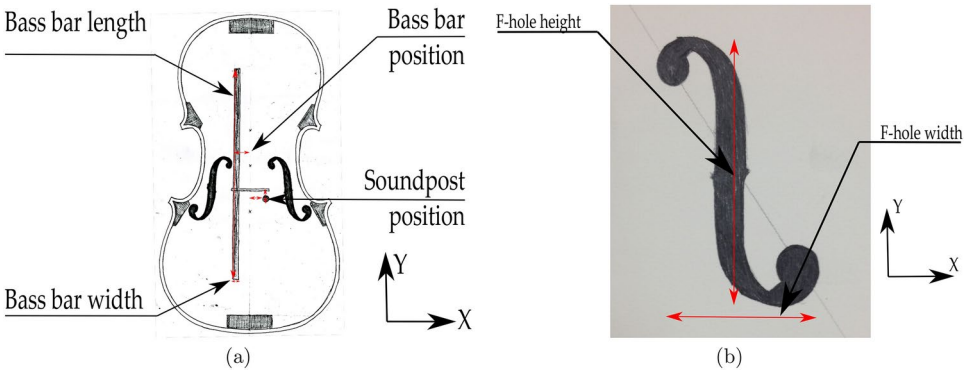

Fig. 10. Close up of the violin soundboard in the XY plane and of the f-holes, the red arrows represent the dimensions that have been modified in the study.

applies the variations of the geometry and material parameters and the updated model is used to compute a new modal basis, and thus new bridge admittance.

Maximum FRF amplitude per frequency band
The maximum value of the Frequency Response Function (FRF) is computed by identifying the highest amplitude of the FRF over the frequency range of interest, either the maximum value from 20 to 4000 Hz, and between 1600 and 3000 Hz that is the usual domain of investigation of the bridge hill) it is calculated as follows:

$$\mathrm{FRF}_{\max} = \max_{\omega} |FRF(\omega)|$$

Along the maximum amplitude value, the corresponding frequency is also given. These two outputs give the variability of the maximum amplitude that can be measured on a bridge of a violin made with variable geometry and materials. The frequency response dispersion highlights the overall amplitude domain that is reached by the many FRF that are computed. It gathers the mean and max values and gives an envelope of the way the material and geometry variability affects the frequency response function of the studied structure. Moreover, the average FRF of all the runs is also given.

Matched eigenfrequency, eigenfrequencies and eigenvector errors
Some features are directly dependent on the modal basis. The eigenmodes of each modal basis of the study are compared with a nominal modal basis of the violin, made with the mean values of each parameter that are changed during the analysis (both material and geometry parameters). The eigenmodes are correlated with a Modal Assurance Criterion (MAC)[72] used to assess the correlation between mode shapes of different cases. It is defined as follows:

$$\mathrm{MAC}(\phi_a, \phi_b) = \frac{|\phi_a^H \phi_b|^2}{(\phi_a^H \phi_a)(\phi_b^H \phi_b)} \tag{6}$$

Where:

- ϕ_a and ϕ_b are the mode shape vectors (eigenvectors) of the two cases being compared.
- ϕ^H denotes the conjugate transpose of the eigenvectors
- The numerator $|\phi_a^H \phi_b|^2$ represents the squared magnitude of the inner product of the two mode shapes, indicating their correlation.
- The denominator $(\phi_a^H \phi_a)(\phi_b^H \phi_b)$ normalizes the result using the norms of the mode shape vectors, ensuring that the MAC value ranges from 0 to 1.A MAC value of 1 indicates that the mode shapes are identical for all the eigenvector components. 0 indicates that the mode shapes are completely different (orthogonal).

To ensure consistency in the comparison of different geometrical configurations within the finite element model (FEM), we implemented a procedure that aligns geometrical points in the global coordinate frame with the FEM mesh whose indexes may change between each geometrical configuration. These points were paired with corresponding nodes in the FEM mesh with a positional tolerance of less than 5 mm. This tolerance ensures that nodes used for mode shape comparisons remain in close proximity across different geometrical configurations, despite any variations in the mesh. The selected tolerance is much smaller-by a factor of 10 to 20-than the smallest wavelengths of flexural waves in the back and top plates, which range between 5 cm and 10 cm at the highest frequency considered (4000 Hz). These wavelengths correspond to the radial and longitudinal directions of the wood, respectively. The minimum value that is retained for the matching of two modes is 0.6.. Considering

the main changes that can occur between two numerical cases and the sensitivity of the MAC criterion, this allows the matching of many modes between two studies. When the nominal modal basis and the current modal basis with initial values are compared, all the modes are matched. The matched eigenfrequencies are used to study the sensitivity of the parameters in regard to the eigenfrequency of each mode that is computed. This gives a non-normalized value for each eigenfrequency. The matched eigenfrequencies error (MEE) is used to compare many eigenfrequencies of eigenmodes at the same time. The MEE is a normalized evaluation of the sensitivity of one parameter in relation to one or many eigenfrequencies. The matched eigenvector error (MEVE) is used to compare the eigenvectors of a given mode of a modal basis to another. In this case, this gives a normalized evaluation of the difference in the shape of the modes, through the error of the MAC criterion.

Results post processing
The screening analysis results are post processed to be displayed in Figs. 3, 4, 5, 6. The elementary effects of each parameters for each observable previously described are normalized. EE_i represent the elementary effect of parameter *i* for a given mode/ observable. The percentage contribution of parameter *i* is calculated as:

$$P_i = \frac{EE_i}{\sum_{i=1}^{N} EE_i} \times 100$$

where:

- EE_i is the elementary effect of the *i*-th parameter,
- $\sum_{i=1}^{N} EE_i$ is the sum of the elementary effects for all (N) parameters *i* considered for the given mode/observable,
- P_i is the normalized percentage contribution of the i^{th} parameter.This normalization ensures that the sum of all percentages for a given mode or observable equals 100%. Therefore it is used to assess the relative importance of each parameter.

Data availability
The datasets used and/or analyzed during the current study available from the corresponding author on reasonable request.

Received: 5 January 2024; Accepted: 11 November 2024
Published online: 28 November 2024

References
1. McIntyre, M. & Woodhouse, J. Acoustics of stringed instruments. *Interdiscip. Sci. Rev.* **3**, 157–173. https://doi.org/10.1179/030801878791926128 (1978).
2. Woodhouse, J. The acoustics of the violin: A review. *Rep. Progr. Phys.* **77**, 115901. https://doi.org/10.1088/0034-4885/77/11/115901 (2014).
3. Mclennan, J. E. *The Violin Music Acoustics from Baroque to Romantic*. Ph.D. thesis, The University of New South Wales (2008).
4. Woodhouse, J. The acoustics of "A0-B0 mode matching" in the violin. *Acta Austica* **84**, 947–956 (1998).
5. Bissinger, G. Wall compliance and violin cavity modes. *J. Acoust. Soc. Am.* **113**, 1718–1723. https://doi.org/10.1121/1.1538199 (2003).
6. Chaigne, A. Recent advances in vibration and radiation of musical instruments. *Flow Turbul. Combust.* **61**, 31–41. https://doi.org/10.1023/A:1026480600366 (1999).
7. Luke, J. Measurement and analysis of body vibrations of a violin. *J. Acoust. Soc. Am.* **49**, 12489. https://doi.org/10.1121/1.1912489 (1971).
8. Jansson, E. V. An investigation of a violin by laser speckle interferometry and acoustical measurements. *Acta Acustica United Acustica* **29**, 21–28 (1973).
9. Reinicke, W. & Cremer, L. Application of holographic interferometry to vibrations of the bodies of string instruments. *J. Acoust. Soc. Am.* **48**, 988–992. https://doi.org/10.1121/1.1912237 (1970).
10. Bissinger, G. Modal analysis of a violin octet. *J. Acoust. Soc. Am.* **113**, 2105–2113. https://doi.org/10.1121/1.1555614 (2003).
11. Bissinger, G. & Keiffer, J. Radiation damping, efficiency, and directivity for violin normal modes below 4 kHz. *Acoust. Res. Lett. Online* **4**, 7. https://doi.org/10.1121/1.1524623 (2003).
12. Weinreich, G., Holmes, C. & Mellody, M. Air-wood coupling and the Swiss-cheese violin. *J. Acoust. Soc. Am.* **108**, 2389–2402. https://doi.org/10.1121/1.1314397 (2000).
13. Le Conte, S., Le Moyne, S. & Ollivier, F. Modal analysis comparison of two violins made by A. Stradivari. *Acoustics* **2012**, 2743–2747 (2012).
14. Fabre, B., Gilbert, J., Hirschberg, A. & Pelorson, X. Aeroacoustics of musical instruments. *Annu. Rev. Fluid Mech.* **44**, 1–25. https://doi.org/10.1146/annurev-fluid-120710-101031 (2012).
15. Hutchins, C. M. The physics of violins. *Sci. American* **207**, 78–93 (1962).
16. Hutchins, C. M. The acoustics of the violin plates. *Sci. American* **245**, 1–11. https://doi.org/10.1038/scientificamerican1081-170 (1981).
17. Hutchins, C. M. & Voskuil, D. Mode tuning for the violin maker. *CAS J.* **2**, 5–9 (1993).
18. Casazza, M. et al. A procedure for the characterization of a music instrument vibro-acoustic fingerprint: The case of a contemporary violin. *Acta IMEKO* **12**, 1445. https://doi.org/10.21014/actaimeko.v12i3.1445 (2023).
19. Gough, C. Vibrational modes of the violin family. In *Proceedings of the Stockholm Music Acoustics Conference, SMAC* **2013**, 66–74 (2013).
20. Weinreich, G. Violin radiativity: Concepts and measurements. In *Proceedings SMAC-Stockholm Music Acoustics Conf.* 99 – 110 (Royal Swedish Academy of Music, 1985).
21. Weinreich, G. & Arnold, E. B. Method for measuring acoustic radiation fields. *J. Acoust. Soc. Am.* **68**, 404–411. https://doi.org/10.1121/1.384751 (1980).

22. Vos, H. J., Warusfel, O., Misdariis, N. & de Vries, D. Analysis and reproduction of the frequency spectrum and directivity of a violin. *J. Acoust. Soc. Neth.* **167**, 1–11 (2003).
23. Jansson, E. V., Niewczyk, B. K., Fryden, L., Niewczyl, B. & Fryden, L. Timbre and properties of the violin. *EPJ Web Conf.* **6**, 28004. https://doi.org/10.1051/epjconf/20100628004 (2010).
24. Fiocco, G. et al. Compositional and morphological comparison among three coeval violins made by giuseppe guarneri "del Gesù" in 1734. *Coatings* **11**, 1–13. https://doi.org/10.3390/coatings11080884 (2021).
25. Woodhouse, J. The physics of the violin. *Contemp. Phys.* **27**, 61–62. https://doi.org/10.1080/00107518608210998 (1986).
26. Jansson, E. V. Admittance measurements of 25 high quality violins. *Acta Acustica United Acustica* **83**, 337–341 (1997).
27. Zhang, C. Z., Zhang, G. M., Ye, B. Y. & Liang, L. D. Violin bridge mobility analysis under in-plane excitation. *Sensors (Switzerland)* **13**, 15290–15306. https://doi.org/10.3390/s131115290 (2013).
28. Merhar, M. & Humar, M. The influence of wood modification on transfer function of a violin bridge. *Drvna Industrija* **71**, 163–169. https://doi.org/10.5552/drvind.2020.1966 (2020).
29. Lämmlein, S. L. et al. Frequency dependent mechanical properties of violin varnishes and their impact on vibro-mechanical tonewood properties. *Results Mater.* **2020**, 100137. https://doi.org/10.1016/j.rinma.2020.100137 (2020).
30. Malvermi, R. et al. The impact of alkaline treatments on elasticity in spruce tonewood. *Sci. Rep.*[SPACE]https://doi.org/10.1038/s41598-022-17596-z (2022).
31. Brémaud, I., Gril, J. & Thibaut, B. Anisotropy of wood vibrational properties: Dependence on grain angle and review of literature data. *Wood Sci. Technol.* **45**, 735–754. https://doi.org/10.1007/s00226-010-0393-8 (2011).
32. Buen, A. The Humidity Experiment - How wood and the violin are affected by variation in humidity . https://doi.org/10.13140/RG.2.2.26226.04806 (2019).
33. Bissinger, G. *Modal Analysis Comparison of New Violin Before and After -250 Hours of Playing* 822–827 (2015).
34. Nastac, S. M. et al. Correlation between acoustic analysis and psycho-acoustic evaluation of violins. *Appl. Sci.* **12**, 8620. https://doi.org/10.3390/app12178620 (2022).
35. Mihalcica, M. et al. Experimental modal analysis of violin bodies with different structural patterns of resonance spruce. *IOP Conf. Ser.*[SPACE]https://doi.org/10.1088/1757-899X/1182/1/012048 (2021).
36. Gough, C. The violin: Chladni patterns, plates, shells and sounds. *Eur. Phys. J.* **145**, 77–101. https://doi.org/10.1140/epjst/e2007-00149-0 (2007).
37. Pyrkosz, M. A. *Reverse Engineering the Structural and Acoustic Behavior of a Stradivari Violin*. Ph.D. thesis, Michigan Technological University (2013).
38. Knott, G. A. *A Modal Analysis of the Violin Using MSC/NASTRAN and PATRAN*. Ph.D. thesis, Naval Postgraduate School, Monterey (1987).
39. Rodgers, O. E. & Masino, T. R. The effect of wood removal on bridge frequencies. *CASJ Catgut Acoust. Soc. J.* **1**, 6–10 (1990).
40. Rodgers, O. E. The effect of the elements of wood stiffness on violin plate vibration. *CASJ Catgut Acoust. Soc. J.* **1** (1988).
41. Gonzalez, S., Salvi, D., Baeza, D., Antonacci, F. & Sarti, A. A data-driven approach to violin making. *Sci. Rep.* **1**, 10. https://doi.org/10.1038/s41598-021-88931-z (2021).
42. Gonzalez, S., Salvi, D., Antonacci, F. & Sarti, A. Eigenfrequency optimisation of free violin plates. *J. Acoust. Soc. Am.* **149**, 1400–1410. https://doi.org/10.1121/10.0003599 (2021).
43. Davis, E. B. On the Effective Material Properties of Violin Plates. In *Proceedings of the Stockholm Music Acoustic Conference 2013, SMAC 2013* 9–15 (Stockholm, 2013).
44. Coffey, J. The Air Cavity , f-holes and Helmholtz Resonance of a Violin or Viola (2013).
45. Nia, H. T. *Acoustic Function of Sound Hole Design in Musical Instruments*. Ph.D. thesis, Massachusetts institute of technology (2010).
46. Nia, H. T. et al. The evolution of air resonance power efficiency in the violin and its ancestors. *Proc. R. Soc. A* **471**, 1–15. https://doi.org/10.1098/rspa.2014.0905 (2015).
47. Molin, N. E., Tinnsten, M. & Wiklund, U. A Violoinmaker's Practical Test Of Wood Properties Suggested From FEM Analysis Of An Orthotropic Shell. *JCAS* **46** (1986).
48. Viala, R., Placet, V. & Cogan, S. Simultaneous non-destructive identification of multiple elastic and damping properties of spruce tonewood to improve grading. *J. Cult. Heritage* **42**, 108–116. https://doi.org/10.1016/j.culher.2019.09.004 (2020).
49. Viala, R., Cabaret, J., Sedighi-gilani, M., Placet, V. & Cogan, S. Effect of indented growth rings on spruce wood mechanical properties and subsequent violin dynamics. *Holzforschung* (2024).
50. Akar, Ö. & Willner, K. Investigating the modal behavior of a violin top and a back plate. *Conf. Proc. Soc. Exp. Mech. Ser.* **8**, 37–44. https://doi.org/10.1007/978-3-031-05445-7_5 (2023).
51. Viala, R., Placet, V. & Cogan, S. Identification of the anisotropic elastic and damping properties of complex shape composite parts using an inverse method based on finite element model updating and 3D velocity fields measurements (FEMU-3DVF): Application to bio-based composite violin sou. *Composites Part A* **106**, 91–103. https://doi.org/10.1016/j.compositesa.2017.12.018 (2018).
52. Viala, R., Placet, V. & Cogan, S. Model-based evidence of the dominance of the guitar brace design over material and climatic variability for dynamic behaviors. *Appl. Acoust.* **182**, 108275. https://doi.org/10.1016/j.apacoust.2021.108275 (2021).
53. Duerinck, T. et al. Experimental comparison of various excitation and acquisition techniques for modal analysis of violins. *Appl. Acoust.* **177**, 107942. https://doi.org/10.1016/j.apacoust.2021.107942 (2021).
54. Gough, C. Acoustic Characterization of Violin Family Signature Modes By Internal Cavity Measurements. In *SMAC 13 Stockholm* 75–81 (2013).
55. Jansson, E. V. Violin frequency response - Bridge mobility and bridge feet distance. *Appl. Acoust.* **65**, 1197–1205. https://doi.org/10.1016/j.apacoust.2004.04.007 (2004).
56. Jansson, E. V. & Barczewski, R. On the Violin Bridge-Hill - Comparison of Experimental Testing and FEM. *Vib. Phys. Syst.* **27** (2016).
57. Woodhouse, J. On the Bridge-Hill of the Violin. *Acta Acustica United Acustica* **91**, 155–165 (2005).
58. Almanza, V. *et al.* Physics-based simulations for assessing the playability of heritage musical instruments: Impact of the soundboard assembly process on its low frequency behavior. *Appl. Acoust.* 1–19 (2023).
59. Viala, R., Placet, V., Cogan, S. & Foltête, E. Model-based effects screening of stringed instruments. In *Conference Proceedings of the Society for Experimental Mechanics Series* **3**, 151–157. https://doi.org/10.1007/978-3-319-29754-514 (2016).
60. Bissinger, G. A0 and A1 coupling, arching, rib height, and f-hole geometry dependence in the 2 degree-of-freedom network model of violin cavity modes. *J. Acoust. Soc. Am.* **104**, 3608. https://doi.org/10.1121/1.423943 (1998).
61. Gough, C. Violin plate modes. *J. Acoust. Soc. Am.* **137**, 139–153. https://doi.org/10.1121/1.4904544 (2015).
62. Bös, J. Numerical optimization of the thickness distribution of three-dimensional structures with respect to their structural acoustic properties. *Struct. Multidiscip. Optim.* **32**, 12–30. https://doi.org/10.1007/s00158-005-0560-y (2006).
63. Yu, Y., Jang, I. G., Kim, I. K. & Kwak, B. M. Nodal line optimization and its application to violin top plate design. *J. Sound Vib.* **329**, 4785–4796. https://doi.org/10.1016/j.jsv.2010.05.022 (2010).
64. Viala, R., Placet, V. & Cogan, S. Model-based quantification of the effect of wood modifications on the dynamics of the violin. *International Symposium on Music Acoustics, ISMA 2019* (2019).
65. Fritz, C. et al. Soloist evaluations of six Old Italian and six new violins. *Proc. Natl. Acad. Sci. USA* **111**, 7224–7229. https://doi.org/10.1073/pnas.1323367111 (2014).

66. Viala, R. *Towards a model-based decision support tool for stringed musical instrument making*. Ph.D. thesis, Université Bourgogne Franche-comté (2018).
67. Guitard, D. & El Amri, F. Modèles prévisionnels de comportement élastique tridimensionnel pour les bois feuillus et les bois résineux. *Ann. Sci. For.* **44**, 335–358 (1987).
68. Cornelius, L. Lanczos1950 (1950).
69. Sprossmann, R. et al. Characterization of acoustic and mechanical properties of common tropical woods used in classical guitars. *Results Phys.* **7**, 1737–1742. https://doi.org/10.1016/j.rinp.2017.05.006 (2017).
70. Morris, M. D. Factorial sampling plans for preliminary computational experiments. *Technometrics* **33**, 161–174. https://doi.org/10.2307/1269043 (1991).
71. Li, Q., Huang, H., Xie, S., Chen, L. & Liu, Z. An enhanced framework for Morris by combining with a sequential sampling strategy. *Int. J. Uncertain. Quantif.* **13** (2023).
72. Allemang, R. J. & Brown, D. L. A correlation coefficient for modal vector analysis. In *First International Modal Analysis Conference* 110–116 (Orlando, 1982).

Acknowledgements

The authors acknowledge Maurice BEAUFORT, a French luthier, and more generally luthiers from the ALADFI and GLAAF groups for their many fruitful discussions and comments.

Author contributions

R.V. has made the computations, complementary experiments and written the paper. V.P. has directed the work and reviewed results and method and corrected the manuscript, S.C. has initiated and directed the overall work, reviewed the results and method and corrected the manuscript. E.F. has obtained funding for the PhD thesis associated with this work.

Additional information

Correspondence and requests for materials should be addressed to R.V.

Reprints and permissions information is available at www.nature.com/reprints.

Publisher's note Springer Nature remains neutral with regard to jurisdictional claims in published maps and institutional affiliations.